Eur. Phys. J. D **43**, 147–150 (2007)
DOI: 10.1140/epjd/e2007-00089-5

THE EUROPEAN PHYSICAL JOURNAL D

Structure and electronic properties of a heterojunction between a single wall carbon nanotube and a TiC cluster

N. Fujima[1,a], R. Tamura[1], and T. Oda[2]

[1] Faculty of Engineering, Shizuoka University, Hamamatsu 432-8561, Japan
[2] Graduate School of Natural Science and Technology, Kanazawa University, Kanazawa 920-1192, Japan

Received 24 July 2006 / Received in final form 29 September 2006
Published online 24 May 2007

Abstract. Atomic structures and electronic properties of heterojunctions of Ti-TiC and TiC-single wall carbon nanotube, Ti_{48}-$Ti_{19}C_{26}$ and $Ti_{19}C_{24}$-C_{30}, are studied by the first principles calculation based on the density functional theory. At the junctions, these substrates are smoothly connected with each other and keep their original structures and electronic properties. The structures of the junctions obtained in the present work give a realistic model to ab initio study for electronic transport properties through the junction of a carbon nanotube and an electrode.

PACS. 31.15.Ar Ab initio calculations – 61.46.Bc Clusters – 61.46.Fg Nanotubes – 73.20.-r Electron states at surfaces and interfaces

1 Introduction

The junction or connection between carbon nanotubes (CNT) and metal electrodes has been one of the most attractive problems both in nanodevice technology and in mesoscopic science since CNT became a candidate for conducting wires at the nanoscale.

To find low resistance ohmic contacts to CNT, a lot of studies have been performed for many kinds of metal electrode, such as Ni, Nb, and Ti [1–9]. Among the several candidates for the electrode, it is known that titanium has good properties, high electrical conductance and good contact to CNT [6,8,9].

Zhang et al. have reported that TiC is formed at the interface between a CNT and a Ti substrate by a heating treatment, that TiC nanorods contacting with the CNTs are grown during the heating process, and that the nanojunction has a linear resistance lower by one-fifth to one-third than the value before heating [1]. They have also shown high-resolution TEM images of the nanojunctions, that give helpful information for building an atomic-scale model of the heterostructure. TiC itself has a unique combination of properties, high conductivity, high hardness and high melting point, and is expected to be utilized for high-technology materials. Then, it is very interesting to study the junctions to TiC.

In the present paper, we assume a model for Ti-TiC-CNT heterojunctions based on the previous works, optimize the structure by ab initio calculations, and discuss their electronic properties. The Ti-TiC-CNT model will be used for study the electronic transport properties through such a heterojunctions in the future work.

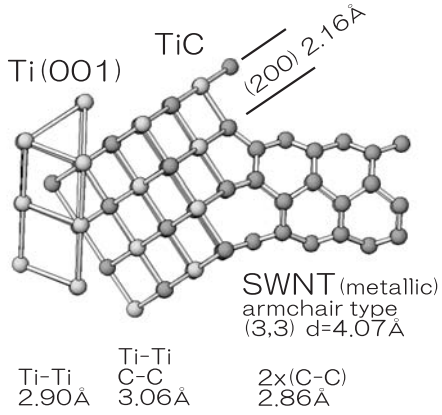

Fig. 1. A model for Ti-TiC-SWNT heterojunction.

2 Ti-TiC-SWNT model

We propose a candidate model for heterostructures of junctions of Ti-TiC-CNT based on high-resolution TEM images [1].

In the model, as shown in Figure 1, a (111) surface of a NaCl-type TiC is connected to a hcp-Ti(001) surface, and the opposite surface of TiC to an armchair-type single wall carbon nano tube (SWNT) with a chiral vector (3,3). As a result, Ti, TiC and SWNT are interfaced under a three-fold symmetry.

[a] e-mail: tsnfuji@ipc.shizuoka.ac.jp

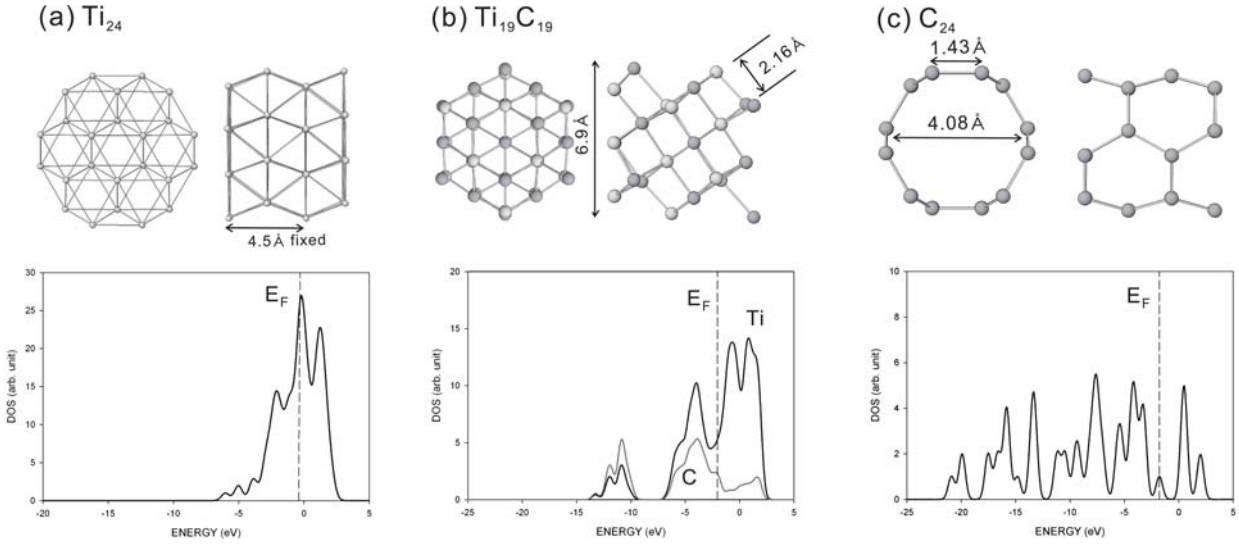

Fig. 2. The optimized atomic structures and PDOSs of simple rods constituting the junctions, (a) hcp-Ti_{24}, (b) NaCl-type $Ti_{19}C_{19}$ and (c) (3,3)-C_{24}.

At the interfaces of Ti-TiC, the regular triangles of the Ti lattice are connected in the mismatch of 5% for the ideal lattice (Ti-Ti distance is 2.90 Å for hcp-Ti, 3.06 Å for TiC). At the interfaces of TiC-SWNT, a regular hexagon of C with a center atom is connected with six atoms of (3,3)-C in the mismatch of 7% (C-C distance for TiC is 3.06 Å, and a diagonal distance of a hexagon of the SWNT is 2.86 Å).

The center C atom of the hexagon in TiC is removed as discussed in Section 5. Employing this model as the initial structure, we individually optimized the heterojunctions of Ti-TiC and TiC-SWNT.

3 Calculations

We perform two types of calculations; (1) periodic junction of rods in a super cell, and (2) isolated junction of clusters (CNT).

(1) All calculations for the systems with the periodic boundary along the junction axis, are performed with VASP (Vienna Ab-initio Simulation Package), a plane-wave based density functional calculation package [10]. We employ the ultrasoft pseudopotential for the core orbitals [11] (1s for C and 1s-3p for Ti) under the generalized gradient approximation (PW91 [12]). The cutoff energy for the plane wave basis is 181.2 eV (NORMAL precision in VASP).

Ti_{48}(hcp-Ti) connected with (111) surface of $Ti_{19}C_{26}$ (NaCl-type) cluster, and $Ti_{19}C_{24}$ connected with (3,3) SWNT C_{30} are taken as the model of junctions. Atomic structures are fully optimized in a supercell by varying the length along the junction axis. The length of more than 15 Å is taken for the other cell axes to avoid the boundary influence. The Γ point approximation is applied during structure optimization.

Simple nanorods of Ti_{24}, $Ti_{19}C_{19}$, and C_{24} are also employed for comparison with the junction.

(2) To clarify local structures at the terminal, we also calculate the heterostructures of non periodic (isolated) systems by ADF(Amsterdam Density Functional) package [13], where the exchange-correlation energy is estimated by the generalized gradient approximation (VWN [14] + PW91). We use the TZP STO-basis with frozen cores of the 1s orbital for C atoms and of the 1s-2p orbitals for Ti atoms. We discuss the structures of C atoms at the terminal or the interface for $Ti_{19}C_{26}$ (NaCl type TiC) and $Ti_{19}C_{25or26}$+C_{30} SWNT. Optimizations are restricted within the three-fold symmetry.

4 Results

In Figure 2, we show the optimized atomic structures and the partial density of states (PDOS) of simple rods (1-dimensionally continuous substances) that constitute the heterojunctions in Figure 1: (a) hcp-Ti_{24}, (b) NaCl-type $Ti_{19}C_{19}$, and (c) (3,3) C_{24} in a supercell. They show typical geometrical and electronic characters, (we do not discuss them here) and are used as the reference for the heterojunctions. All the PDOSs in Figure 2 and in the following figures are cut about at 2 eV.

4.1 Ti-TiC heterojunction

In this junction, the C-(111) surface of TiC is connected with the (001) surface of hcp-Ti along the three-fold axis. Figure 3 shows the optimized atomic structures and PDOS of the Ti-TiC heterojunction, hcp-Ti_{48} and NaCl-type $Ti_{19}C_{26}$. Because the lattice parameters of Ti for hcp-Ti and for TiC are similar to each other and TiC is an interstitial compound, Ti_{48} and $Ti_{19}C_{26}$ are smoothly connected and the atomic structures are almost kept after the connection (e.g. lattice parameter of 2.1–2.2 Å for (200) in TiC).

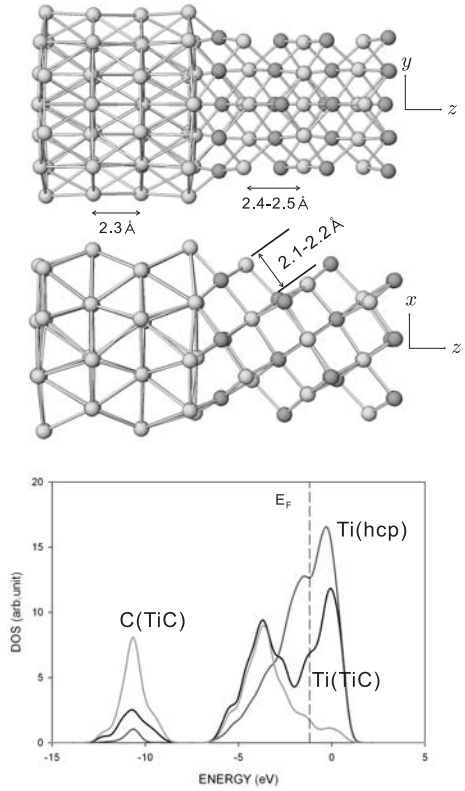

Fig. 3. The optimized atomic structure and PDOSs of Ti-TiC heterojunction, Ti_{48}-$T_{19}C_{26}$.

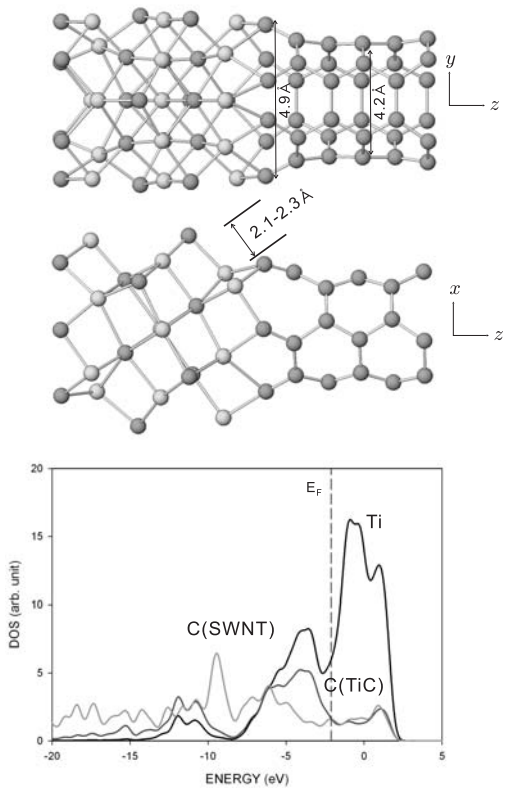

Fig. 4. Optimize structure and PDOSs of TiC-SWNT heterojunction, $Ti_{19}C_{24}$-C_{30}.

By charge transfer from hcp-Ti, PDOSs of C and Ti (TiC) in occupied states are enlarged.

4.2 TiC-SWNT heterojunction

In this junction, we remove a C atom at the center of both surfaces (terminals) of $Ti_{19}C_{26}$ as discussed in the following section. Figure 4 shows the optimized structure and the PDOSs of the junction, $Ti_{19}C_{24}$ and C_{30}.

The diameter of C hexagons at the surface of TiC is 4.9 Å, which slightly shrinks from that of the simple TiC, but still larger than that of the (3,3)-SWNT. Then the diameter of SWNT at the middle region also enlarges about 0.1 Å in comparison with those of simple (3,3)-C rods.

The NaCl structure of the TiC is still kept although it is distorted more than that for the Ti-TiC junction in Figure 3 and the lattice parameter of (200) varies from 2.1 to 2.3 Å. The PDOS of TiC is very similar to that of the simple TiC rod in Figure 2.

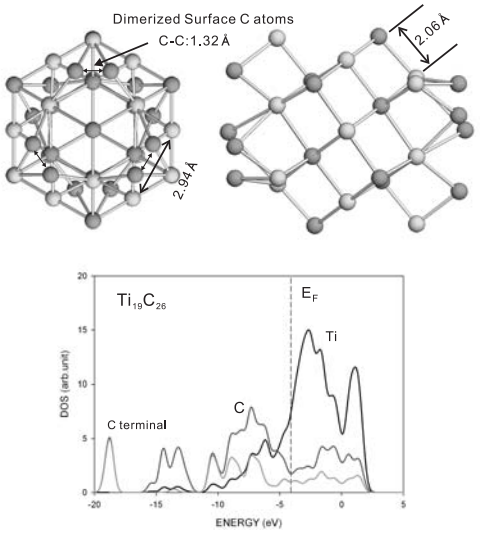

Fig. 5. Optimized structure and PDOS of isolated $Ti_{19}C_{26}$ cluster.

5 Discussions

5.1 C dimerization

Figure 5 shows the optimized structure of an isolated NaCl-type $Ti_{19}C_{26}$ cluster, where both the ends are terminated by seven C atoms (6 hexagon, 1 center). The optimized structure indicates that the terminal C atoms are dimerized with an interatomic distance of 1.32 Å. As a result, the structure except the center atom becomes similar to a ring of the C(3,3)-SWNT, and the PDOS profile of the terminal C atoms in Figure 5 is close to that of a SWNT in Figure 4 rather than that in TiC.

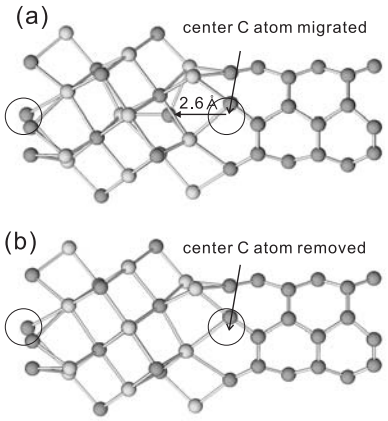

Fig. 6. Optimized structure of isolated TiC clusters connected with C_{30}-SWNT, (a) $Ti_{19}C_{56}$ and (b) $Ti_{19}C_{55}$.

Then, it is expected that the TiC cluster is smoothly connected with the (3,3)-SWNT by the dimerization. However, the dimerization may appear on the edge of a cluster or on a small substrate. We will have to verify how the dimerization occurs on larger surface.

5.2 C migration

Connecting a C(3,3)-SWNT with the $Ti_{19}C_{26}$ cluster at the terminal discussed above, the center C atom at the junction migrates into the TiC by more than 2.5 Å as shown in Figure 6a. The migration causes the NaCl-type TiC some complicated structure. (It is noted that the structure in Figure 6 seems not so complicated because the restriction of the three-fold symmetry is applied so that the center atom moves only along the three-fold axis. We have obtained more complicated structures without the symmetry restriction.) C atoms easily migrate into the TiC substrate because TiC is an interstitial compound and the dimerization around the center, that is, formation of a SWNT with small diameter repulses the center atom. Figure 6b shows the optimized structure of the $Ti_{19}C_{55}$ in which the center atom at the junction has been removed in advance. By removing the center atom, the original structure is well kept.

It is also noted that the optimized structure by isolated calculation in Figure 6b is very similar to that by the periodic calculation in Figure 4 although the latter is fully optimized in a super cell whereas the former is done under the three-fold symmetry restriction. This fact that the calculations with different manners have obtained similar results suggests a reliability of calculations and the model.

6 Conclusions

We calculate the atomic structures and electronic properties of the heterojunctions of a Ti-TiC cluster and TiC-SWNT, such as Ti_{48}-$Ti_{19}C_{26}$ and $Ti_{19}C_{24}$-C_{30}. Although these clusters are very small, their characters of atomic and electronic structures are well-defined and keep their original characters at the junctions. Therefore the Ti-TiC-SWNT model employed here may be a candidate of a realistic model to study the junctions of CNT and Ti electrode by the first principles approach. In the future works, we modify (simplify) the present junction model and apply it to study for electronic transport properties by using a tight-binding calculation with Green's function approach such as Laudauer's formula [15,16].

References

1. Y. Zhang, T. Ichihashi, E. Landree, F. Nihey, S. Iijima, Science **285**, 1719 (1999)
2. H. Dai, J. Kong, C. Zhou, N. Franklin, T. Tombler, A. Cassell, S. Fan, M. Chpline, J. Phys. Chem. **103**, 11246 (1999)
3. C. Zhou, J. Kong, H. Dai, Appl. Phys. Lett. **76**, 1597 (1999)
4. C. Zhou, J. Kong, H. Dai, Phys. Rev. Lett. **84**, 5604 (2000)
5. M. Menon, A.N. Andriotis, G.E. Froudakis, Chem. Phys. Lett. **320**, 425 (2000)
6. Y. Zhang, N.W. Franklin, R.J. Chen, H. Dai, Chem. Phys. Lett. **331**, 35 (2000)
7. C. Yang, J. Zhao, J. Lu, Phys. Rev. B **66**, R041403 (2002)
8. J.J. Palacios, A.J. Pérez-Jiménez, E. Louis, E. SanFabián, J.A. Vergés, Phys. Rev. Lett. **90**, 106801 (2003)
9. Y. Liu, Phys. Rev. B **68**, 193409 (2003)
10. VASP 4.6, University Vienna
11. D. Vanderbilt, Phys. Rev. B **41**, 7892 (1996)
12. J.P. Perdew, J.A. Chevary, S.H. Vosko, K.A. Jackson, M.R. Pederson, D.J. Singh, C. Fiolhais, Phys. Rev. B **46**, 6671 (1991)
13. ADF2005.01, Scientific Computing and Modelling
14. S.H. Vosko, L. Wilk, M. Nusair, Canadian J. Phys. **58**, 1990 (1220)
15. S. Datta, *Electrnic Transport in Mesoscopic Systems* (Cambridge Univ. Press, Cambridge, 1995)
16. S. Kokado, N. Fujima, K. Harigaya, H. Shimizu, A. Sakuma, Phys. Rev. B **73**, 172410 (2006)